Acta Cryst. (1970). A26, 140

Crystal Structures of Three Polytypes of Lead Iodide: Correlation Between Phenomena of Arcing and Polytypism

BY V. K. AGRAWAL, G. K. CHADHA AND G. C. TRIGUNAYAT
Department of Physics and Astrophysics, University of Delhi, Delhi-7, India

(*Received* 4 *February* 1969)

An X-ray study of single crystals of lead iodide grown by the gel method has revealed that the arcing phenomenon occurs rarely in this compound. The polytypism is also not observed frequently. The arcing phenomenon originates from arrangements of partial or unit edge-dislocations created during crystal growth. On the basis of Jagodzinski's disorder theory the polytypism can also be explained in terms of partial edge dislocations. Thus, the two phenomena appear to be interrelated. The complete crystal structures of three PbI_2 polytypes, 10*H*, 14*H* and 20*H*, have been computed. These are found to be $(11)_3 22$, $(11)_5 22$ and $(11)_7 2112$, respectively, in Zhdanov symbols, with space group P3*m*1. Their formation can be explained in terms of partial edge dislocations created at regular intervals, providing further support to the possibility of the polytypism and arcing phenomena being mutually related.

Introduction

Subsequent to the frequent observation of the arcing phenomenon (Agrawal & Trigunayat, 1969*a*,*b*), which consists of an extension of diffraction spots into small arcs, in the polytypic crystals of cadmium iodide, it was proposed to investigate lead iodide crystals which have a similar MX_2-type of structure and are also known to have a polytypic character (Hanoka, Vedam & Henisch, 1967). The crystals have been grown by the gel-method and an X-ray investigation of a large number of them has revealed that the arcing phenomenon rarely occurs in these crystals. The occurrence of polytypes is also less frequent in comparison with CdI_2 crystals, which points to the possibility of the arcing and polytypism phenomena being related to each other. The arcing phenomenon owes its origin to the creation of partial or unit edge-dislocations during growth (Agrawal & Trigunayat, 1969*a*). Polytypism in crystals can also be explained in terms of partial edge dislocations, creating stacking faults, as proposed by Jagodzinski (1954*a*) and substantiated in the subsequent experimental studies on silicon carbide (Jagodzinski, 1954*b*) and cadmium iodide (Jain & Trigunayat, 1968). Thus, the two phenomena may be correlated. The detailed atomic structures of three new polytypes, 10*H*, 14*H* and 20*H*, of lead iodide have been worked out to provide more information regarding this correlation.

Experimental methods

The crystals were grown in silica gel (Mitchell, 1959). Sodium silicate of specific gravity 1·06, *N* acetic acid and *N* lead acetate were gelled in a test tube and covered with a 2*N* potassium iodide solution. Hexagonal and trigonal crystal platelets of lead iodide, up to 3 mm across and 0·2 mm in thickness, grew after two days under ordinary room conditions. They could be easily retrieved from the gel for subsequent investigations.

The optically perfect single crystals were subjected to X-ray examination. A cylindrical camera of radius 3 cm and a collimator of aperture 0·5 mm were used. The size of the focal spot was 1 mm^2. The crystals were mounted along the *a* axis. The range of oscillation was from 25° to 40°, *i.e.* the *c* axis made an angle of 25–40° with the incident X-ray beam. This range yielded a large number of 10.*l* reflexions due to only one of the faces, upper or lower, of a crystal platelet (Chadha & Tigunayat, 1967). Laue photographs were also taken with the X-ray beam incident in the direction of the *c* axis. For the determination of structures, zero layer *a* axis Weissenberg photographs (5·73 cm camera diameter) were taken and the observed intensities for 10.*l* reflexions were compared with the corresponding calculated intensities (Mitchell, 1959).

Experimental results and structure determination

Sixty PbI_2 crystals were subjected to X-ray examination. As the crystals sometimes displayed syntactic coalescence, diffraction spots from the two faces of a crystal were separately recorded giving rise to double the number, *viz.* 120, of oscillation photographs. Only six of them have shown arcing. Two representative examples are presented in Figs. 1 and 3, where X-ray reflexions are seen to spread into arcs, each consisting of two spots lying one above the other and joined by a faint strip between them. In Fig. 1, which is the oscillation photograph of a mixture (4*H*+10*H*) of polytypes, the arcing exists for reflexions of the 4*H* type alone. The Laue photographs of four crystals displayed a similar arcing as on the corresponding oscillation photographs. One of the remaining two crystals showed small closed ring-shaped reflexions on its Laue photograph and the other showed U-shaped reflexions. All such cases of arcing, and more, have already been observed in CdI_2 crystals (Agrawal & Trigunayat, 1969*a*,*b*).

The majority of the crystals were found to be the

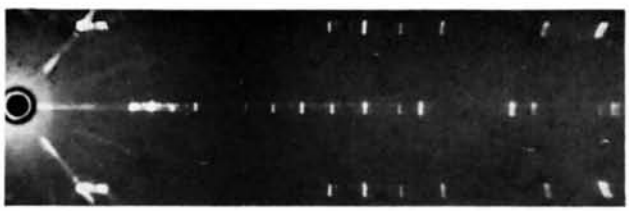

Fig. 1. *a*-axis 15°-oscillation photograph of the first crystal. Cu $K\alpha$ radiation, camera diameter 6 cm.

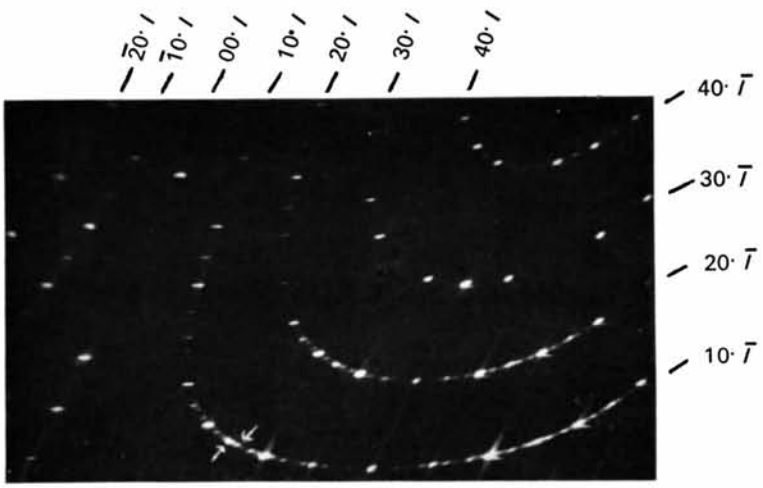

Fig. 2. Zero layer *a*-axis Weissenberg photograph of the first crystal, Cu $K\alpha$ radiation; camera diameter 5·73 cm. The arrow marks on the upper and lower sides, respectively, of the 10.*l* festoon indicate the reflexions 10·7 and 10·3 of $10H$ and $4H$, respectively. The *l* value of the lowest spot on the 10.*l* festoon is zero.

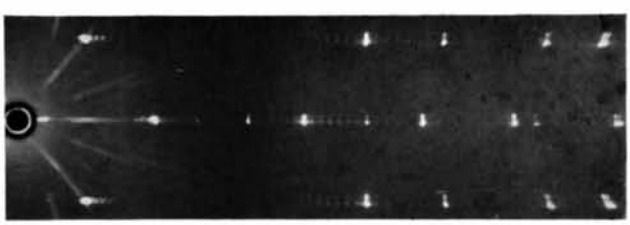

Fig. 3. *a*-axis 15°-oscillation photograph of the second crystal; other conditions as in Fig. 1.

[*To face p.* 140

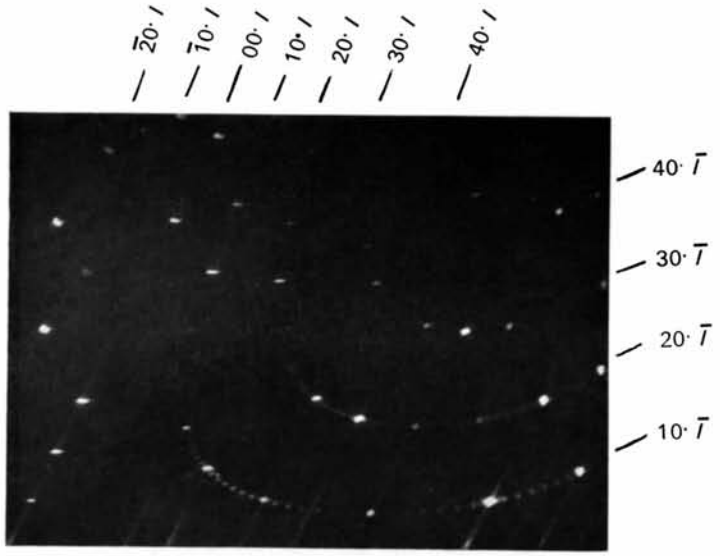

Fig. 4. Zero layer *a*-axis Weissenberg photograph of the second crystal; other conditions as in Fig. 2. The *l* value of the lowest spot on the 10.*l* festoon is zero.

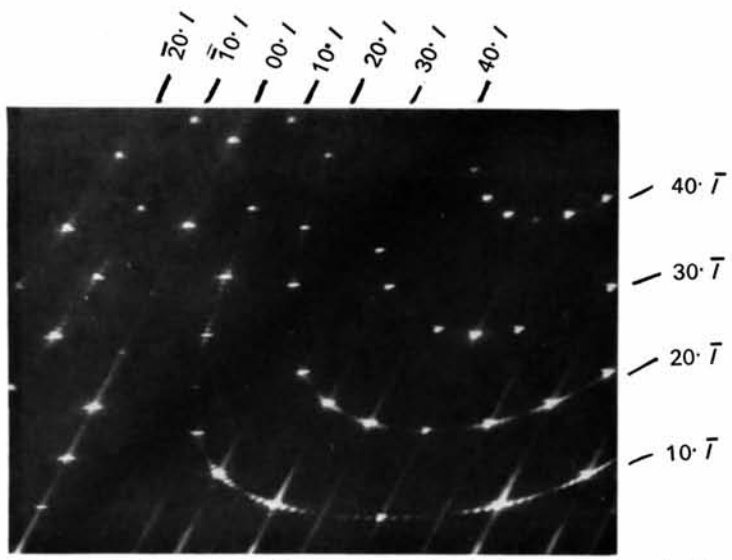

Fig. 5. Zero layer *a*-axis Weissenberg photograph of the third crystal; other details as in Fig. 4.

common type $2H$. A few crystals of types $4H$ and $12R$ have also been observed. The crystal structures of these three types have been determined earlier (Terpstra & Westenbrink, 1926; Mitchell, 1959). Three higher polytypes, *viz.* $10H$, $14H$ and $20H$, were also observed. The polytypes of the same c dimensions as the first two have been reported earlier by Hanoka *et al.* (1967) without determining their crystal structures, but the present ones could be different types by virtue of different stacking sequences of layers in their structures. The third one, *viz.* $20H$, has not been reported earlier. The crystal structures of these three types have been worked out as follows:

Polytype $10H$

In the structure determination of the three PbI_2 polytypes, the cell dimensions of the basic type $2H$, built up by the repetition of a single 'minimal sandwich', have been taken to be $a=b=4{\cdot}557$ and $c=6{\cdot}979$ Å, as determined by Swanson, Gilfrich & Ugrinic (1955). The ionic positions are:

1 Pb at $(\frac{1}{3},\frac{2}{3},z)$
2 I at $(0,0,0)$; $(\frac{2}{3},\frac{1}{3},2z)$

where, $z=0{\cdot}265$ (Mitchell, 1959).

The polytype $10H$ occurred in coalescence with type $4H$ and an unidentified type. The a-axis oscillation photograph (Fig. 1) and the zero layer a-axis Weissenberg photograph (Fig. 2) of the crystal show mixed diffraction spots of these types. The respective indices of the spots due to the types $4H$ and $10H$ have been indicated in Fig. 2. Except for an overlapping with alternate $4H$-positions, the $10H$-spots are quite distinct on account of their shapes. The positions of overlapping, widely spaced as they are, hardly interfere in the structure determination. The spots of the unidentified type do not interfere either, as these are very weak and have a different characteristic shape. There are fifteen possible ways in which layers can be stacked to form a ten-layered hexagonal structure. The intensity calculations for all of them were made for $10.l$ reflexions by using the formula

$$I\propto\{\sum_{ZA,\alpha} f_{I,Pb}\cos 2\pi lz+\sum_{ZP,\beta} f_{I,Pb}\cos 2\pi(lz-\tfrac{1}{3})+\sum_{ZC,\gamma} f_{I,Pb}\cos 2\pi(lz+\tfrac{1}{3})\}^2+\{\sum_{ZA,\alpha} f_{I,Pb}\sin 2\pi lz+\sum_{ZB,\beta} f_{I,Pb}\sin 2\pi(lz-\tfrac{1}{3})+\sum_{ZC,\gamma} f_{I,Pb}\sin 2\pi(lz+\tfrac{1}{3})\}^2 \quad (1)$$

where z_A, z_B, z_C, denote the respective z coordinates of the iodine (Roman letters) and lead (Greek letters) ions on the vertical A,B,C axes, respectively, passing through $(0,0,0)$, $(\frac{2}{3},\frac{1}{3},0)$ and $(\frac{1}{3},\frac{2}{3},0)$, respectively. $\sum_{ZA,\alpha}$ represents the summation over iodine ions at A sites and lead ions at α sites, similar expressions being used for the other summations. The values of I for different l values, obtained from equation (1) are multiplied by the Lorentz–polarization factor $(1+\cos^2 2\theta)/\sin 2\theta$, where θ is the Bragg angle. A good agreement between the observed and calculated intensities was obtained for the structure $(11)_3 22$ alone. The observed and calculated intensities are given in Table 1. The intensities were compared only from 10.0 to 10.20 (except for $l=0$, 10, 20, which coincide with $4H$-positions).

The detailed structure of $10H$ is therefore as follows.
Space group $P3m1$
Cell dimensions $a=b=4{\cdot}557$, $c=34{\cdot}895$ Å
Zhdanov symbol $(11)_3 22$
ABC sequence: $(A\gamma B)$ $(A\gamma B)$ $(A\gamma B)$ $(A\gamma B)$ $(C\alpha B)$
Atomic coordinates:

4 iodine atoms at $0,0,n_1z'$
5 iodine atoms at $\frac{2}{3},\frac{1}{3},(n_2z'+2z)$
1 iodine atom at $\frac{1}{3},\frac{2}{3},16z'$
4 lead atoms at $\frac{1}{3},\frac{2}{3},(n_3z'+z)$
1 lead atom at $0,0,(16z'+z)$

where $n_1/4$, $n_2/4$ and $n_3/4$ have integral values from 0 to 3, 0 to 4, and 0 to 3, respectively, $z'=1/20$, and $z=0{\cdot}265/5$.

Polytype $14H$

This polytype occurred in syntactic coalescence with the common type $2H$. Figs. 3 and 4 are the respective a axis oscillation and zero-layer Weissenberg photographs of the crystal. Starting from first principles and using all the Zhdanov numbers, *prima facie* the structure determination appears to be a difficult task. Theoretically, there can be 2^{13} possible ways of arranging

Table 1. *Observed and calculated relative intensities for* $10.l$ *reflexions of polytype* $10H$

$10.l$	Observed intensity	Calculated intensity	$10.l$	Observed intensity	Calculated intensity
0	*vs**	78·7	11	*ms*	150·8
1	*w*	26·8	12	*m*	121·7
2	*mw*	51·2	13	*mw*	92·7
3	*m*	86·2	14	*w*	65·5
4	*ms*	124·8	15	(*vvs**)†	766·8
5	*vvs**	167·4	16	(*a*)	24·8
6	*s*	187·5	17	(*a*)	12·7
7	*s*	202·7	18	(*a*)	6·3
8	*s*	205·1	19	(*a*)	4·3
9	*s*	195·6	20	(*s**)	4·5
10	*vvs**	1000			

* These spots overlap with $4H$-positions. Therefore, their intensity values are not reliable.
† The reflexions in parentheses lie in the high absorption region.

a 14-layered structure. However, upon examining the intensity sequence of the 10.*l* spots, it is revealed that the intense diffraction spots of this type either coincide with the spots of the common type 2*H* having structure (11), or lie around them, indicating that its unit cell must mostly consist of (11) units. Thus, the crystal structure could possibly be one of the following three:

(1) 11 11 11 11 11 22
(2) 11 11 11 11 2 11 2
(3) 11 11 11 2 11 11 2 .

The calculated intensities for the 10.*l* reflexions for these structures were compared with those observed on the Weissenberg photograph (Fig. 4). An excellent agreement between the calculated and observed values, given in Table 2, was obtained for the first structure, *viz.* $(11)_5 22$. As in the previous case, the intensities were compared for the spots 10.0 to 10.28 alone.

The detailed structure of 14*H* is therefore as follows.
Space group $P3m1$
Cell dimensions $a=b=4{\cdot}557$, $c=48{\cdot}853$ Å
Zhdanov symbol $(11)_5 22$
ABC sequence: $(A\gamma B)$ $(A\gamma B)$ $(A\gamma B)$ $(A\gamma B)$ $(A\gamma B)$ $(A\gamma B)$ $(C\alpha B)$
Atomic coordinates:

6 iodine atoms at $0,0,n_1z'$
7 iodine atoms at $\frac{2}{3},\frac{1}{3},(n_2z'+2z)$
1 iodine atom at $\frac{1}{3},\frac{2}{3},24z'$
6 lead atoms at $\frac{1}{3},\frac{2}{3},(n_3z'+z)$
1 lead atom at $0,0,(24z'+z)$

where $n_1/4$, $n_2/4$ and $n_3/4$ are integers and have values 0 to 5, 0 to 6, and 0 to 5, respectively, $z'=0/28$, and $z=0{\cdot}265/7$.

Polytype 20*H*

This polytype was found to occur in coalescence

Table 2. *Observed and calculated relative intensities for* 10.*l reflexions of polytype* 14*H*

10.*l*	Observed intensity	Calculated intensity	10.*l*	Observed intensity	Calculated intensity
0	*ms**	79·4	15	*mw*	67·1
1	*vvw*	9·6	16	*mw*	58·6
2	*vw*	15·1	17	*mw*	49·7
3	*w*	23·6	18	*w*	40·7
4	*w*	34·2	19	*w*	32·4
5	*mw*	45·8	20	*vw*	24·7
6	*mw*	57·5	21	(*ms**)†	724·0
7	*ms**	72·2	22	(*a*)	12·4
8	*m*	76·5	23	(*a*)	8·0
9	*m*	82·9	24	(*a*)	4·9
10	*m*	86·3	25	(*a*)	2·9
11	*m*	86·8	26	(*a*)	2·0
12	*m*	84·9	27	(*a*)	1·9
13	*m*	80·6	28	(*a**)	1·8
14	*vvs**	1000			

* These spots overlap with 2*H*-positions. Therefore, their intensity values are not reliable.
† The reflexions in parentheses lie in the high absorption region.

Table 3. *Observed and calculated relative intensities for* 10.*l reflexions of polytype* 20*H*

10.*l*	Observed intensity	Calculated intensity	10.*l*	Observed intensity	Calculated intensity
0	*vs**	78·7	21	*ms*	148·4
1	*w*	18·4	22	*m*	98·7
2	*w*	17·6	23	*w*	44·8
3	*vw*	12·9	24	*vvw*	9·2
4	*vvw*	4·9	25	*a*	0
5	*a*	0	26	*a*	8·8
6	*vvw*	8·2	27	*vw*	27·1
7	*mw*	36·4	28	*w*	42·8
8	*m*	81·7	29	*w*	48·2
9	*ms*	129·7	30	(*vs**)†	766·7
10	*vvs**	167·5	31	(*vvw*)	29·7
11	*ms*	158·7	32	(*a*)	16·2
12	*ms*	122·8	33	(*a*)	6·2
13	*m*	68·0	34	(*a*)	1·2
14	*vw*	19·4	35	(*a*)	0
15	*a*	0	36	(*a*)	0·6
16	*vw*	19·6	37	(*a*)	1·6
17	*m*	69·6	38	(*a*)	2·8
18	*ms*	128·1	39	(*a*)	4·4
19	*ms*	168·9	40	(*mw**)	88·5
20	*vvs**	1000			

* These spots overlap with 2*H*-positions. Therefore, their intensity values are not reliable.
† The reflexions in parentheses lie in the high absorption region.

with the type 2*H*. Fig. 5 is the zero layer *a* axis normal beam Weissenberg photograph of the crystal showing 10.*l* and 10.$\bar{l}$ spots around the central Laue streak. The intensity distribution of 10.*l* spots bears a marked similarity to that of the type 14*H*, indicating once again that the structure must contain a large number of (11) units. Thus, the possible structure could be one of the following:

(1) 11 11 11 11 11 11 11 11 22
(2) 11 11 11 11 11 11 11 2 11 2
(3) 11 11 11 11 11 11 2 11 11 2
(4) 11 11 11 11 11 11 22 22 .

The structure (2) showed an excellent agreement between the calculated and observed intensity values, listed in Table 3. As in the earlier cases, the intensities for reflexions 10.0 to 10.40 alone were compared.

The detailed structure of 20*H* is therefore as follows.
Space group $P3m1$
Cell dimensions $a=b=4{\cdot}557$, $c=69{\cdot}79$ Å
Zhdanov symbol $(11)_7 2112$

ABC sequence: $(A\gamma B)$ $(A\gamma B)$ $(A\gamma B)$ $(A\gamma B)$ $(A\gamma B)$ $(A\gamma B)$ $(A\gamma B)$ $(A\gamma B)$ $(C\alpha B)$ $(C\alpha B)$

Atomic coordinates:

8 iodine atoms at $0,0,n_1z'$
10 iodine atoms at $\frac{2}{3},\frac{1}{3},(n_2z'+2z)$
2 iodine atoms at $\frac{1}{3},\frac{2}{3},n_3z'$
8 lead atoms at $\frac{1}{3},\frac{2}{3},(n_4z'+z)$
2 lead atoms at $0,0,(n_5z'+z)$

where $n_1/4$, $n_2/4$, $n_3/4$, $n_4/4$ and $n_5/4$ have integral values from 0 to 7, 0 to 9, 8 to 9, 0 to 7, and 8 to 9, respectively, $z'=1/40$, and $z=0{\cdot}265/10$.

Discussion

The 'minimal sandwich', consisting of a layer of lead ions sandwiched between two close-packed layers of iodine ions, of lead iodide structures, is isostructural with the 'minimal sandwich' of cadmium iodide structures. All polytypes of these substances are built up by piling various numbers of these sandwiches into various arrangements. Consequently, the likely slip planes and slip directions in PbI_2 crystals should be the same as those in CdI_2 crystals. The processes of creation of partial or unit edge-dislocations, and their arrangements into macroscopically vertical tilt boundaries should also be similar. Such processes have already been observed and explained in CdI_2 crystals (Agrawal & Trigunayat, 1969*a*). A tilt boundary divides the crystal into two blocks, making each reflexion on the X-ray photograph extend into a small arc. The arc is made up of two spots, each due to one of the blocks, connected by a strip arising from the distorted region between the blocks. Illustrations are provided in Figs. 1 and 3. In Fig. 1 the arcing is seen to occur only for the spots of polytype 4*H*, showing that the edge dislocations were profusely created during the growth of this type alone. The combined effect of a number of boundaries parallel to different vertical planes can give rise to composite figures of various shapes on the X-ray photographs, as earlier observed in CdI_2 crystals. Two such cases have been encountered in the present work as well (photographs not reproduced).

A theory of polytypism in terms of an ordering of stacking faults, resulting from the creation of partial edge dislocations, has been advanced by Jagodzinski (1954*a*). As the force needed to move a dislocation is necessarily less than the force required to create it, a partial edge dislocation can easily move along the basal plane up to the end of the crystal, shifting an entire layer into a new position, *i.e.* creating a stacking fault. The theory provides for the creation of stacking faults at a regular interval of layers during crystal growth, the ordering effect of the faults being provided by vibration entropy. The theory has been verified for the case of strongly polytypic crystals of silicon carbide, by Jagodzinski (1954*b*) himself, and for cadmium iodide by Jain & Trigunayat (1968). The generation of the polytypes whose crystal structures have been determined by us can also be satisfactorily understood on the basis of this theory. The structure 10*H*, $(AB)_4CB$, can be easily generated from the common polytype 2*H* by introducing a stacking fault, which displaces the atoms on an *A* layer to *C* positions, after every ten layers of the crystal. The polytype 14*H*, with the structure $(AB)_6CB$, can be similarly created by introducing a fault after every fourteen layers. For obtaining the third structure, *viz.* $(AB)_8(CB)_2$ of 20*H*, faults have to occur on the first layers of two successive sandwiches at a regular interval of twenty layers.

In the present investigation, only 5% of PbI_2 crystals have shown arcing, in wide contrast to 42% of instances in the case of CdI_2 crystals (Agrawal & Trigunayat, 1969*a*). The relative abundances of polytypes other than the common type (the type 2*H* in PbI_2 and the type 4*H* in CdI_2) are also widely different in the cases of PbI_2 and CdI_2. Only 10% of crystals of PbI_2 happen to be such polytypes, whereas in CdI_2 crystals investigated earlier (Agrawal & Trigunayat, 1969*a*) such polytypes amount to nearly 25%. These large discrepancies can be understood from structural considerations as follows. The distance between adjacent 'minimal sandwiches' in PbI_2 is smaller than that in CdI_2. As an approximate estimate, the van der Waals forces of attraction between two adjacent sandwiches will be inversely proportional to the sixth power of the interatomic distances. Therefore, qualitatively speaking, the forces will be stronger in PbI_2 than in CdI_2. Correspondingly, PbI_2 will need more energy for a slip of layers than in CdI_2, causing the frequency of generation of partial or unit edge-dislocations (depending upon the direction of slip) during growth to become smaller in its case. This explains the observed lesser incidence of arcing and polytypism in PbI_2. Therefore the phenomena of arcing and polytypism can be correlated in terms of edge dislocations.

This work was financially supported by the University Grants Commission and the Council of Scientific and Industrial Research, India. The authors also wish to acknowledge Drs K. D. Chaudhuri and V. P. Duggal for their kind interest and encouragement.

References

AGRAWAL, V. K. & TRIGUNAYAT, G. C. (1969*a*). *Acta Cryst.* A**25**, 401.
AGRAWAL, V. K. & TRIGUNAYAT, G. C. (1969*b*). *Acta Cryst.* A**25**, 407.
CHADHA, G. K. & TRIGUNAYAT, G. C. (1967). *Acta Cryst.* **22**, 573.
HANOKA, J. I., VEDAM, K. & HENISCH, H. K. (1967). *Crystal Growth* (Supplement *J. Phys. Chem. Solids*), p. 369.
JAGODZINSKI, H. (1954*a*). *Acta Cryst.* **7**, 300.
JAGODZINSKI, H. (1954*b*). *Neues Jb. Miner.* **3**, 49.
JAIN, R. K. & TRIGUNAYAT, G. C. (1968). *Z. Kristallogr.* **126**, 153.
MITCHELL, R. S. (1959). *Z. Kristallogr.* **111**, 372.
SWANSON, H. E., GILFRICH, N. T. & UGRINIC, G. M. (1955). *National Bureau of Standards Circular 539.* **5**, 34.
TERPSTRA, P. & WESTENBRINK, H. G. K. (1926). *Proc. Acad. Sci. Amst.* **29**, 431.

Acta Cryst. (1970). A**26**, 144

Van der Waals Interactions and Molecular Packing in Crystals of Cubic α-Nitrogen, Orthorhombic Cyanogen and Monoclinic Octachlorocyclobutane

BY A. DI NOLA AND E. GIGLIO
Laboratorio di Chimica Fisica dell'Istituto Chimico, Università di Roma, Roma, Italy

(*Received* 23 *April* 1969 *and in revised form* 23 *June* 1969)

The potential energy in molecular crystals of α-nitrogen, cyanogen and octachlorocyclobutane is calculated as a function of the unit-cell parameters. Some available potential functions for nitrogen–nitrogen and chlorine–chlorine interactions between non-bonded atoms are tested. The results show a good agreement between the unit-cell parameters obtained by the X-ray diffraction method and those corresponding to the deepest minimum of the potential energy, when suitable potential functions are used.

Introduction

It has previously been shown (Giglio & Liquori, 1967; Giglio, 1969) that when the molecular geometry of a molecular crystal and the crystal parameters and symmetries are known, the crystal packing may be predicted by locating the deepest minima of the intermolecular van der Waals and hydrogen bonding energies, which are computed as a function of all the rotational and translational degrees of freedom defining the coordinates of the asymmetric unit. This method was successfully applied to the determination of the molecular crystal structure of 5α-androstan-3,17-dione (Damiani, Giglio, Liquori & Mazzarella, 1967). Later, the relative validity of the potential functions used was tested in known crystal structures as a function of the unit-cell parameters, considering the molecules as rigid bodies and leaving the crystal symmetries unchanged. Some potential functions, relative to interactions involving hydrogen, carbon, oxygen and sulphur atoms, were verified for crystalline adamantane (Liquori, Giglio & Mazzarella, 1968), orthorhombic sulphur (Giglio, Liquori & Mazzarella, 1968) and polymeric sulphur trioxide (Giglio, Liquori & Mazzarella, 1969).

The results concerning nitrogen–nitrogen and chlorine–chlorine interactions reported here complete a set of potential functions which refer to the more common atoms in organic crystals.

Calculation of van der Waals Potential energy for α-nitrogen and orthorhombic cyanogen

It was decided to test some available nitrogen–nitrogen potential functions: the molecular crystals of α-nitrogen and cyanogen were chosen.

Table 1. *Potential function coefficients for nitrogen–nitrogen interactions*

The energy is in kcal per atom pair (if the interatomic distance is in Å).

Symbol of set	Reference	$A \cdot 10^{-3}$	B	C	D
a	1	387·0	0·000	354	12
b	2	161·0	0·000	363	12
c	3	243·0	0·000	547	12
*d**	4	1439·6	4·010	1557	0
e	5,6	30·1	3·779	232	0
f	5,6	30·1	4·193	124	0

(1) Parsonage & Pemberton, 1967.
(2) Scott & Scheraga, 1966.
(3) Brant, Miller & Flory, 1967.
(4) Mason & Rice, 1954.
(5) Kitaigorodsky, 1961.
(6) Venkatachalam & Ramachandran, 1967.

* Mason and Rice proposed two functions. The first, reported here, fits the crystal properties well and the second Virial coefficients of nitrogen; the second one, which fits the viscosity coefficients, gives very slightly different results.